

---

---

# **Adiabatically tapered fiber-optic microsensor**

- Fabrication and Characterization -

---

---

Capstone 2 Project Report  
Sultan Yelikbayev

Nazarbayev University  
Department of Electrical and Electronics Engineering  
School of Engineering

Copyright © Nazabayev University

Here you can write something about which tools and software you have used for typesetting the document, running simulations and creating figures. If you do not know what to write, either leave this page blank or have a look at the colophon in some of your books.





# NAZARBAYEV UNIVERSITY

**Electrical and Electronics Engineering**

Nazarbayev University

<http://www.nuece.info>

**Title:**

Adiabatically tapered fiber-optic microsensor: Fabrication and Characterization

**Theme:**

Biosensors

**Project Period:**

Spring Semester 2020

**Project Group:**

**Participant(s):**

Sultan Yelikbayev

**Supervisor(s):**

Carlo Molardi

**Copies:** 1

**Page Numbers:** 21

**Date of Completion:**

April 27, 2020

**Abstract:**

As of late, the various techniques from the materials science and biophysics are utilized to study the physical properties of the microstructure of the chemical and biological specimen. Through a considerable many of them give phenomenal sensibility, they have a few requirements concerning electromagnetic interference, fabrication complexity and specific laboratory conditions for operating. Hence, to overcome these constraints the new family of micro-scale fiber optical sensors was introduced. There are several methods to fabricate microfibers with different microtechnology. However, the techniques with more simple, economical and robust fabrication process are still developing. Therefore, this study proposes the fabrication process of widely interested tapered fiber optic microsensor via Laser Splicing System and characterization of produced tapered microfibers in terms of external RI sensitivity. The final product that was achieved is the fiber with the least waist diameter  $19 \mu\text{m}$  has RI sensitivity of  $156.8215 \text{ nm/RIU}$  and agreeable linear correlation between the wavelength shift and RI change. In addition, the detailed fabrication process with characterization method is presented in the following sections. Moreover, the observed trends in fabrication process and recommendations based on the practice experience are also suggested in this report.

*The content of this report is freely available, but publication (with reference) may only be pursued due to agreement with the author.*

# Contents

<b>Preface</b>	<b>vi</b>
<b>1 Introduction</b>	<b>1</b>
1.1 Background Information . . . . .	1
1.2 Significance of the Tapered microscale FOS and its potential . . . . .	2
1.3 Fundamental Physics of Micro-Structured Fiber Optic Sensor . . . . .	4
<b>2 Sensor Fabrication and Characterization</b>	<b>7</b>
2.1 The process of tapered microscale FOS fabrication . . . . .	7
2.2 Testing the RI external sensitivity . . . . .	9
2.3 The Simulation of Light Transmission Intensity by COMSOL . . . . .	15
2.4 Discussions and Recommendations . . . . .	15
<b>3 Conclusion</b>	<b>19</b>
<b>Bibliography</b>	<b>20</b>

# Preface

Here is the preface. You should put your signatures at the end of the preface.

Nazarbayev University, April 27, 2020

---

Sultan.Yelikbayev  
<sultan.yelikbayev@nu.edu.kz>

# Chapter 1

## Introduction

### 1.1 Background Information

In recent decades, a rapid development of the industry requires the expansion of new sensing technologies that provide higher sensibility, simplicity in manufacturing and low cost. In some areas of industry, to be precisely in the energy sector, a high level of electromagnetic fields creates interference in conventional sensors, which prevents accurate measurement of various parameters (e.g. pressure) in various technical systems. A vivid example of this is the low-oil circuit breakers in power plants. In addition, an increase in the global population and life expectancy necessitates the creation and use of new biomedical devices to provide more effective diagnosis, observation and treatment of patients. In this regards, it seems extremely attractive to develop fiber-optic sensors (FOS) systems for various industrial and medical purposes [1]. The main advantage of FOS - insensitivity to electromagnetic and radio frequency signals - makes them ideal for diagnosing patients in real time directly during magnetic resonance imaging and computed tomography, when the use of other types of sensors is problematic [1]. The very small diameter (less than 250 microns) and high flexibility of optical fibers, as well as low losses during the propagation of light create opportunities for the manufacture of ultra-miniature fiber-optic sensors and their installation directly at the place of measurement [2]. Moreover, the use of FOS is promising in those branches of science and technology where high sensitivity of measuring systems to measured parameters is required in combination with the requirements of fire, explosion and electrical safety, insensitivity to external electromagnetic fields and aggressive environments [3].

A wide class of FOS is based on the registration of microdisplacements of a sensitive element under the action of a measured physical quantity [4]. This registration can be carried out using measuring systems of amplitude or interference type. Most FOS with an external primary converter is built according to the scheme

when the measured physical quantity (pressure, temperature, acceleration, etc.) causes the mechanical movement of a certain element (for example, a membrane or inertial mass), which, in turn, leads to modulation of light intensity [4]. In such sensor circuits, optoelectronic mechanical displacement meters play a key role. In other words, FOS can be a universal basis or a basic element of a whole family of sensors of various physical quantities that differ only in the design of the primary transducer.

At the same time, the development of fiber optic sensors received a new impetus using microelectronics technology and microsystem technology. Good opportunities have opened up to miniaturizing FOS and reducing their cost while maintaining high sensitivity. Ongoing improvements in fiber-optic detecting have included blasting exploration in the plan and assembling of novel microscale organized optical fiber sensors and introduced a new class of micro FOS. Recently, there are various fabrication techniques for microscale FOS that can provide novel design and technology platform for exploring the micro world [5]. However, due to their manufacturing complexity and high cost, the new schemes and methods for simple production are popular and consistently in search. Therefore, this study proposes the simple fabrication method for adiabatically tapered microscale FOS and their characterization in terms of refractive index (RI), due to the fact that most biological and chemical specimens are distinguished to their refractive indices.

Tapered optical microfiber can be defined as the optical fiber, which has relatively small micro-wire waist diameter. It commonly provides high contrast between the core RI and sensing media's RI [6]. In addition to the contrast, the tapered microscale FOS has small dimensions, which makes them capable to have a significant fraction of the guided light, thereby increasing sensitivity to ambient changes in the sensing surrounding. The tapered microfibers are formed by the constant heat transfer and consequent stretching of the soft (waist) region of the fiber to submicron scale [7]. The main advantages of the tapered microfiber include fast-response time, large evanescent field and compactness that make it utilization in industry and in medicine efficient [7].

## **1.2 Significance of the Tapered microscale FOS and its potential**

There are different possible applications of the tapered FOS, especially as it was mentioned before; the FOS can be applied in field industry and in medicine. Particularly, it was suggested that tapered microscale FOS can play important role in investigation of biofilms' structure that can be considered as the thin mat, layer (polymicrobial aggregate) that firmly attached to the surface and where microorganisms are assembled to form convenient environment [8]. In other words, it is known that most bacteria exist in nature not in the form of freely floating cells, but

in the form of specifically organized biofilms [9].

The role of microbial biofilms in the occurrence and development of such common diseases as infections associated with vascular catheterization and other gram-positive microorganisms has been reliably proven; infections of heart valves and joint prostheses; periodontitis due to a number of microorganisms in the oral cavity; urinary tract infections detected ; middle ear infections; cystic fibrosis, tuberculosis and orthodontal diseases [10]. All of these diseases are difficult to treat, have a high frequency of relapses and some of them can be fatal. The mechanisms by which microorganisms forming biofilms cause pathological processes in a macroorganism are far from clear. In addition to the tissues of the host organism, microbial biofilms colonize various medical devices of a non-biological nature that are introduced into the human body (catheters, pacemakers, heart valves, orthopedic devices) [11]. Studies of implanted medical devices using electron microscopy have shown the presence of bacterial biofilms. Moreover, biofilms are accountable for biofouling and contamination of process water, deterioration of the hygienic quality of drinking water and microbially influenced corrosion [8]. In addition, there are also severe problems in industrial processing due to the microorganisms and development of biofilm where the water use is required. Accumulation of microorganism by water flow and biofilm formation on the surface of the industrial processing equipment can lead to increased operational cost [12]. Here some of the common industrial problems related to biofilms[13]:

- Decreased efficiency of the heat exchangers that use cooling water to control process-fluid temperatures, because of the reduced heat transfer associated with an accumulation of microorganisms on the surface.
- Accumulation on surfaces that has direct contact with water and designed for human consumption, e.g., drinking water or food products, which can lead health problems.
- Interfering with chemical additives that are used for prevention of metal corrosion can result into undesired response to biofilms
- Damage to cooling water-systems as the result of rise of power loss in water circuits. Accumulated bacteria might create blockade form his slime mass due to biofilm and waste production and enhance the corrosion process
- Occurrence of surface corrosion (including pitting) on the surfaces of process equipment due to bacteria and their microbial metabolism, which can result oxygen depolarization and further inducing the potential difference on metal surfaces. Moreover, there will be produce of insoluble ferric hydroxide and insoluble ferrous sulphide deposits according to availability of different types bacteria species

Therefore, the investigation of biofilms is crucial for both medicine and industry processes, and requires the new development of diagnostic and monitoring technologies. Today, there are several techniques for examination biofilms' structure including microscopic, spectroscopic, electrochemical and piezoelectric techniques [14][15]. The most of them provides accurate data and measurement, but their complexity and technical limitations including electromagnetic interference and requirement of the specific laboratory conditions are the main barriers for commercial production and utilization [16]. For this reason, to overcome these obstacles the use of micro-scale FOS can be one of the solutions that can offer both in-situ investigation and non-destructive monitoring of biofilms.

### 1.3 Fundamental Physics of Micro-Structured Fiber Optic Sensor

Before discussing the fabrication process, the factors that defines the performance of the tapered micro fiber optic sensor should be examined.

**The external RI sensitivity** : The main parameter that defines the performance of the MFs is its external refractive index sensitivity, which can be expressed as [17]:

$$\frac{d\lambda}{dn_{ex}} = \frac{\lambda}{\Gamma} \left( \frac{1}{\Delta n} \frac{d\Delta n}{dn_{ex}} \right) \quad (1.1)$$

where dispersion factor is:

$$\Gamma = 1 - \frac{\lambda}{\Delta n} \frac{d\Delta n}{d\lambda} \quad (1.2)$$

Based on the above equation, it can be seen that RI sensitivity is mainly determined by:

- dispersion factor.
- $\Delta n$ , which is mode index difference between local modes.
- $\frac{d\Delta n}{dn_{ex}}$ , that is the RI-induced variation of the intermodal index.

Moreover, it can be seen that the sensitivity increases as the index difference  $\Delta n$  increases, which have more value when the fiber thickness is more thinner. As the result, the RI sensitivity can be greatly improved by reducing the diameter of fiber. Therefore, it can be said by managing the diameter of the waist region and length of the transition regions the RI sensitivity of particular tapered fiber optic sensor can be controlled.

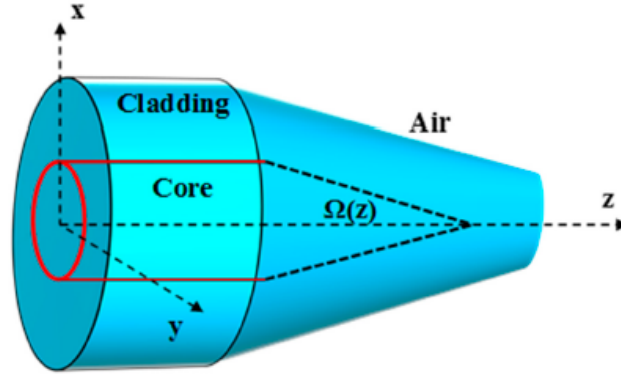


**Figure 1.1:** Schematic diagram of the local tapering angel in transition region

**Low Loss** : Normally the losses (signal to noise ratio) in microfibers are attractively low and mainly related to surface roughness and adiabatic profile (Figure 1.1) [7].

Long fiber tapers, depending on the slope of the taper angle can be categorized as:

1. **Adiabatic** : MFs can be considered as an adiabatic type when there is no transitional power loss and no light energy transfer between the two main local modes. The diameter transition is performed smoothly ensuring a negligible intermodal coupling. In addition, according to Landau-Dykhne formula it was found that optical power losses have exponential dependency on the diameter of fiber in the case of the ideal MF [7].
2. **Non-adiabatic**: For this type, MF has relatively sharp adiabatic angle and during the propagation of the fundamental mode through the optical fiber, it transfers the part of energy to the cladding modes in the taper region. Therefore, there will be several modes propagation along the thinner waist that arise modal interference [7].

Whether the MF is adiabatic or not can be determined from **Adiabatic criterion** [18]:

$$\Omega(z) \leq \frac{r}{z_b} = \frac{r(\beta_1 - \beta_2)}{2\pi} \quad (1.3)$$

where,  $\Omega$  is the angle between the taper radius and longitudinal axis (adiabatic angle),  $z_b$  is beat length, the length required for the polarization to rotate  $360^\circ$ ,  $\beta_1$  and  $\beta_2$  are local propagation constants of the fundamental mode and higher order mode (to which power is most likely to be lost) respectively and  $r$  is a radius of transition region taht is function of  $z$ .

**Evanescent Field** Evanescent field is the essential property that characterizes the fraction of the power that transmits outside the physical MF borderline. Since the MFs designed with strong overlap, the interaction with surrounding environment is not avoidable. The mode interaction extends as guiding power decreases and as the radius of MFs declines. Thus, this expansion continues until it is limited by the cladding and air interface. In extremely small diameters, the modes will be propagated weakly in the evanescent field outside the air and silica interface [7].

Therefore, in order to improve the sensor specificity and sensitivity to selected samples, the MFs are typically coated with particular compounds that are required for corresponding application. For instance, in biological application, the MFs are coated with polymers or resins that are capable of binding specific chemicals during the specimen investigation. In general, it can be said that the MF size plays a crucial role on the field distribution. The fraction of evanescent field power  $\zeta$  can be defined as  $\zeta = 1 - \eta$  where  $\eta$  is a fraction of power that propagates inside the core [19].

**Flexibility** It was mentioned that usually MFs are configured in proper way (like resonators having sharp bends) such that there is negligible bending loss. However, these losses become significant when the diameter of the MFs is lessened to a few microns. For this reason, before the fabrication this bending loss design parameter should be also taken into account. The bending loss coefficient  $\alpha_{bend}$  has the exponential relation with bending radius  $\rho$  and transverse wavenumbers  $U$  and  $V$  [20]:

$$\alpha_{bend} = \frac{U^2}{2VWK_1(W)} \left( \frac{\pi}{r\rho} \right) \exp\left[ -\frac{4W}{3V} \left( 1 - \frac{n_{MF}^2}{n_{surr}^2} \right) \frac{\rho}{r} \right] \quad (1.4)$$

where  $n_{MF}^2$  and  $n_{surr}^2$  are refractive indices of MF and its surrounding medium respectively,  $K_1$  is Bessel function of the second kind.

**Mechanical Strength** The different MFs that are fabricated with various techniques show diverse strength values. For our particular case the taper that is made with adiabatic heating and pull method, the strength values are low and the taper region can be easily broken even during the manufacturing process without properly selected pulling speed. In addition, the taper can be also easily degraded when there is presence of defects and contaminants on the surface. Therefore, before fabrication the fiber should be cleaved.

## Chapter 2

# Sensor Fabrication and Characterization

### 2.1 The process of tapered microscale FOS fabrication

The main technology that was used for the tapered fiber fabrication is Laser Splicing System (LSS) (Fujikura, Inc., LZM-100), which has CO<sub>2</sub> laser heat source instead of electrodes and automatic movement control to provide repeatable production, low maintenance and accuracy. The LSS can be seen from the Figure 2.1. The fiber type that was used for fabrication is single mode fiber (SMF), that are commonly available on the market at the low price and mainly involved in RI measurements. The typical SMF tapered diameter less than 10  $\mu\text{m}$  is capable to achieve a high sensitivity of 980 nm/RIU for a RI range from 1.332 to 1.392, which makes reasonable for the investigation [21].

The working principle of LSS based on the controlling of laser for heating of the waist region of the fiber that is placed between two holders. Then, system moves the right holder by pulling the this soft region with the appointed constant pulling speed to finally produce the tapered region Figure 2.2.

Before placing the SMF with 250  $\mu\text{m}$  cladding and 9  $\mu\text{m}$  core into LSS, its cladding was decreased into 150  $\mu\text{m}$ . The surface of the fiber was cleaned with simple alcohol and then placed into LSS. Then, the LSS was configured with selecting proper values for different parameters such as pulling (drawing) speed, X/Y alignment resolution and taper shape, etc. The taper shape was chosen as sine to provide smooth transition and to reduce the power loss. Specification of operating configuration of LSS:

1. Single mode fiber (SMF)
2. X/Y alignment resolution: 0.1  $\mu\text{m}$



Figure 2.1: Laser Splicing System (LSS), Fujikura LZM -100

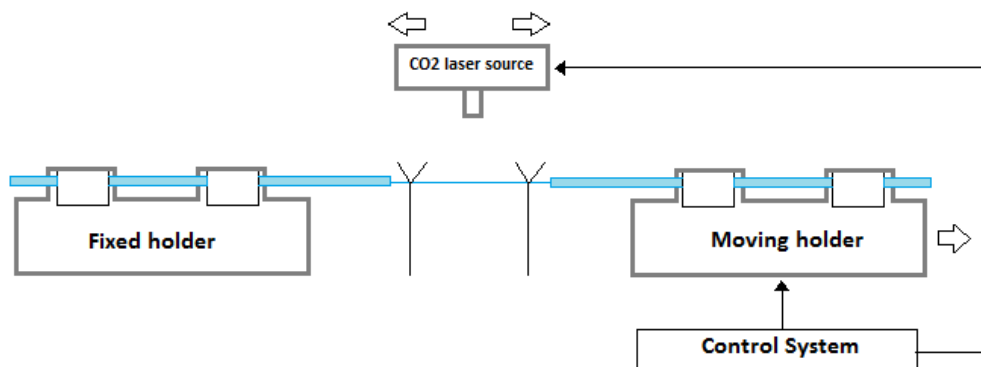


Figure 2.2: The fabrication technique of LSS

3. Z travel Resolution:  $0.125\mu\text{m}$
4. Taper length: 100mm
5. Taper shape: sine

The different tapered fibers with various length and waist diameter were produced. The Table 2.1 displays the five fabricated tapered fibers with designed diameter and actual diameters after the process. The LSS parameters for particular fiber can be also seen from the Table 2.1 including designed length (transition region/uniform waist region/transition region), heating of the laser, calibration points, movement speed of the right holder. The diagram of the tapered fiber with narrowed diameter can be observed from the Figure 2.3. It can be seen that tapered fibers consist of two transition regions on both sides and uniform region on the middle. Actually, it should be denoted the final product might have slightly different length parameters (transition and uniform region length) from the initially designed conditions. The least tapered waist diameter is  $19\ \mu\text{m}$  that was obtained from the designed diameter  $18\ \mu\text{m}$ .

**Table 2.1:** Fabricated tapers with parameters

Designed Length (mm)	Designed Diameter( $\mu\text{m}$ )	Heating	Calibration points	Movement (mm/s)	Actual Diameter( $\mu\text{m}$ )
6/20/6	25	148/50	592	0.42	25
5/10/5	20	151/27	602	0.47	20
12/15/12	18	151/27	602	0.49	20
10/15/10	18	148/42	582	0.49	19
10/15/10	19	156/43	622	0.45	21

**Figure 2.3:** Fiber Optic Sensor Configuration

## 2.2 Testing the RI external sensitivity

The external RI sensitivity testing of the fabricated tapered fibers was conducted by using an optical backscatter reflectometer (Luna, Inc., OBR 4600). The products were tested in different solutions of sucrose by examining the scattered power loss within the tapered region. Figure 2.4.a displays the testing scheme including OBR system, tapered SMF and sucrose solution.

The splicer (Fujikura, Inc., 41S) was used to connect the one end of the fiber with the reflectometer. Further, the fiber's tapered region was submerged into the sucrose solution, which is also in the pre-modified bottle cup that has two pinholes to pass the fiber wires. It was consistently checked and full immersion of tapered fiber is preserved, as shown in Figure 2.4.b. Initially the taper was tested in 10000  $\mu\text{l}$  of 10% solution that as taken as a reference. Afterwards, the 40% sucrose with additional 100  $\mu\text{l}$  was poured into the cup in every step of the testing. For the all tapers the wavelength spectrum was taken from the 1525nm to 1610nm. The spectrum wavelength shift for the 25  $\mu\text{m}$  tapered FOS can be viewed from the Figure 2.5.a.

The sensitivity is determined by tracing the wavelength shift of a selected resonance in the transmission spectrum versus RI change and can be observed from the Figure 2.5.b. For all tapers the interested region of RI from 1.347 (sucrose 10%) to 1.35377 (sucrose 10% + 1000 $\mu\text{l}$  sucrose 40%).

The RI sensitivity for the particular tapered FOS 247.8258nm/RIU with the coefficient of determination  $R^2 = 0.68555$ . For the perfect result the the obtained

system.png

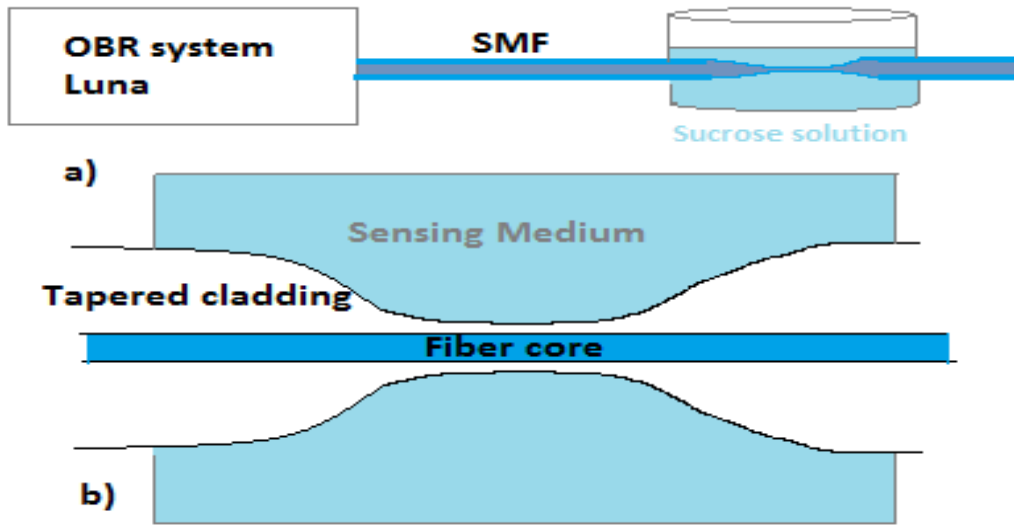


Figure 2.4: OBR testing system diagram

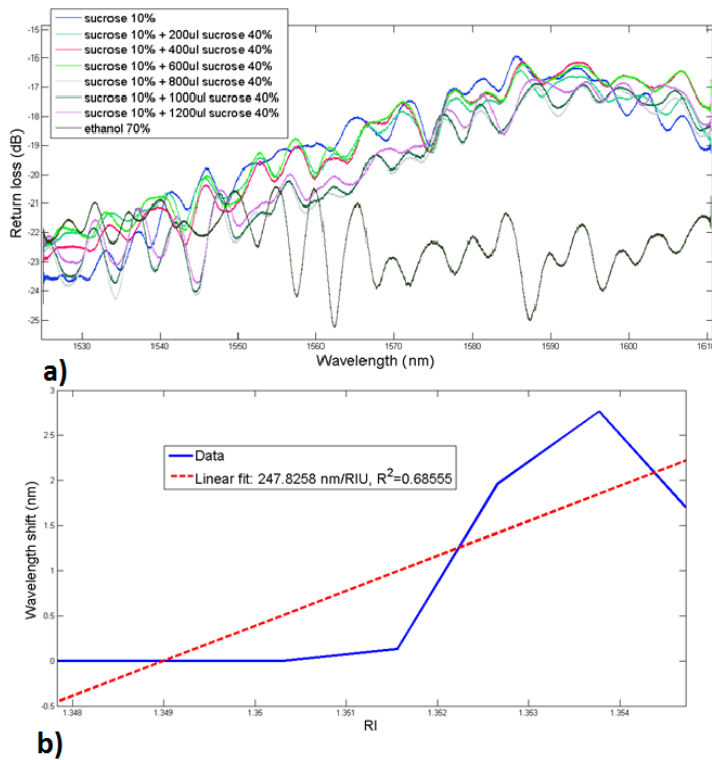
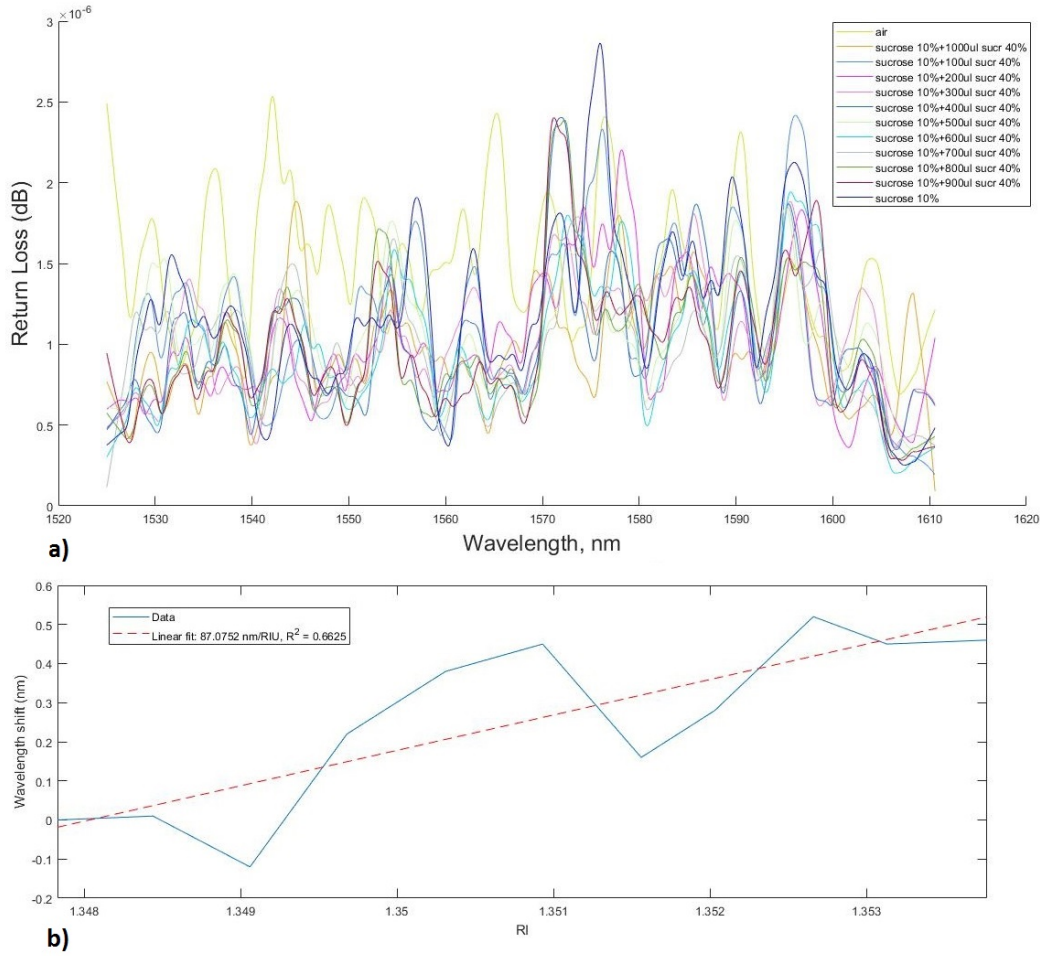


Figure 2.5: Tapered FOS with waist diameter 25 $\mu$ m: a) Spectrum of the wavelength shift; b) Wavelength shift as a function of the RI change

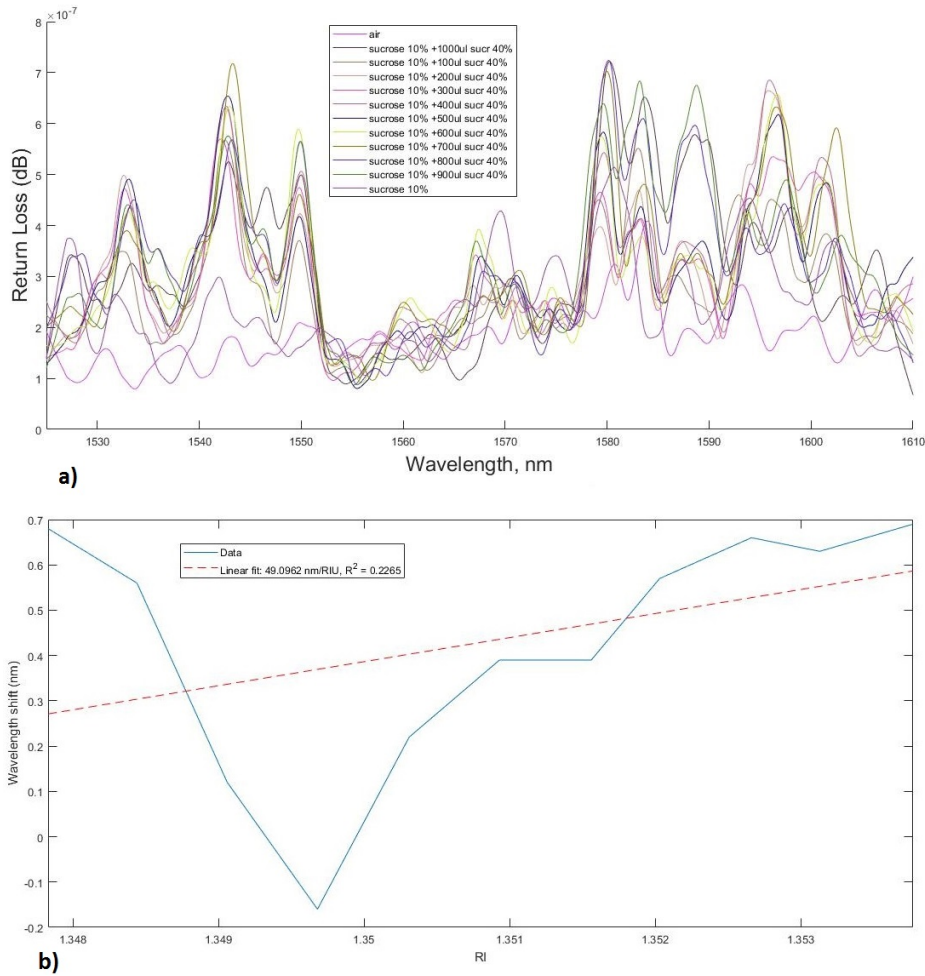


**Figure 2.6:** Tapered FOS with waist diameter  $21\mu\text{m}$ : a) Spectrum of the wavelength shift; b) Wavelength shift as a function of the RI change

data should be match with linear fit ( $R^2 = 1$ ).

Figure 2.6 displays the spectrum of the wavelength shift and its change with respect to RI change for tapered FOS with waist diameter  $21\mu\text{m}$ . Here The RI sensitivity is equal to  $87.0752\text{ nm/RIU}$  with the coefficient of determination  $R^2 = 0.6625$ . The decrease if the waist diameter slightly decreased the coeffic. of determination and gradually declined the RI sensitivity. While in fact, the decrease of the waist diameter should increase the sensitivity. The main reason is that the cladding was not totally removed. There is still some submicron cladding material.

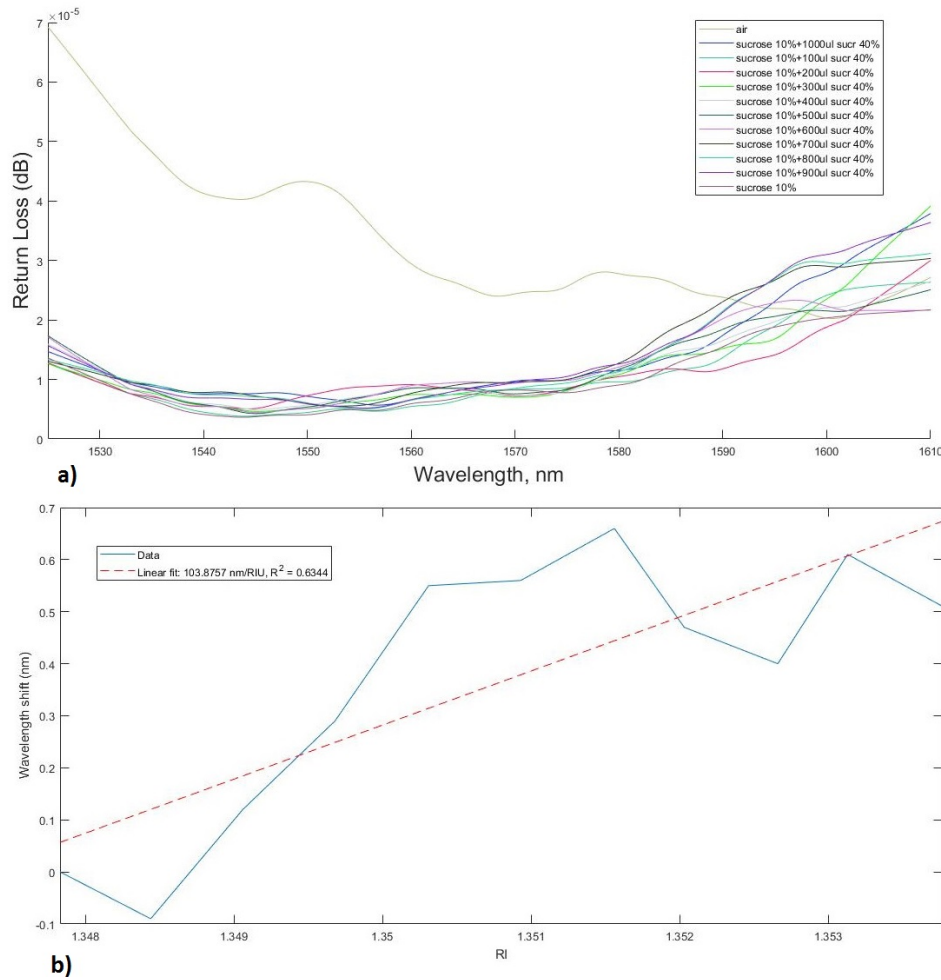
The return loss spectrum of of the tapered SMF with  $20\mu\text{m}$  and tapered length  $20\text{mm}$  was computed by OBR system, as shown in Figure2.7.a. The resulted sensitivity of the product is  $49.0962\text{ nm/RIU}$  with coeffic. of determination  $R^2 = 0.2265$ . The low sensitivity and poor linearity could be the outcome of the sharp transition



**Figure 2.7:** Tapered FOS with waist diameter  $20\mu\text{m}$  and length 20mm: a) Spectrum of the wavelength shift; b) Wavelength shift as a function of the RI change

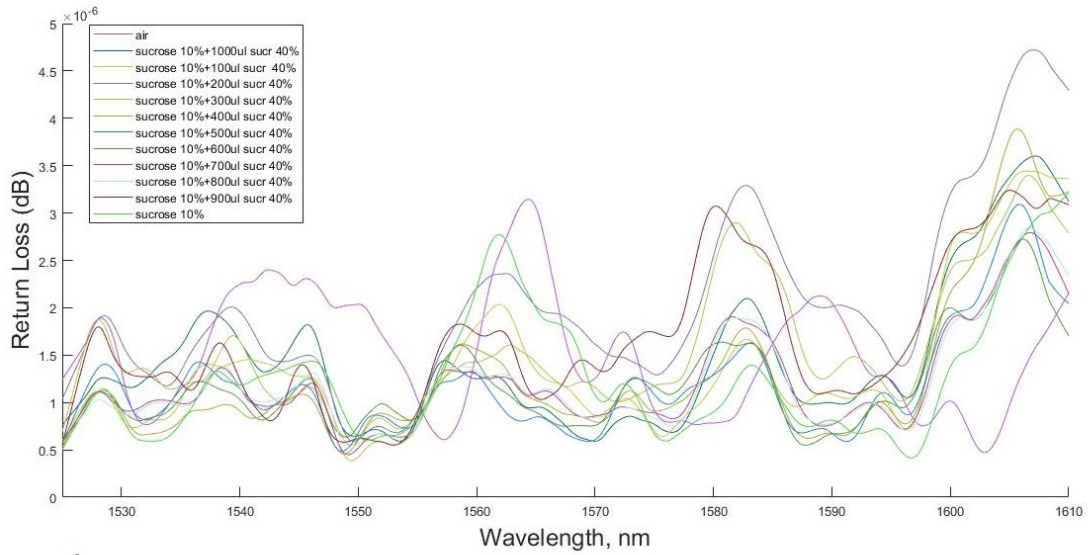
(relatively small transition length 5mm) from the waist diameter and cladding diameter, consequently formation of high adiabatic (tapering) angle. As the result, relatively great transitional power loss. Therefore, the second taper with same parameters but with increased transition length was fabricated and tested in term of RI sensitivity.

Figure 2.8 shows the spectrum of the wavelength shift and its change with respect to RI change for tapered FOS with waist diameter  $20\mu\text{m}$  and length 39mm including uniform length 15mm and transitional length 12mm at the both sides. The product has increased sensitivity of 103.8757 nm/RIU with improved linearity  $R^2 = 0.6344$ . As the mentioned before, the decrease of the tapering angle by increasing the transition is the main factor of the enhancement of the both sensitivity and linearity of the fiber.

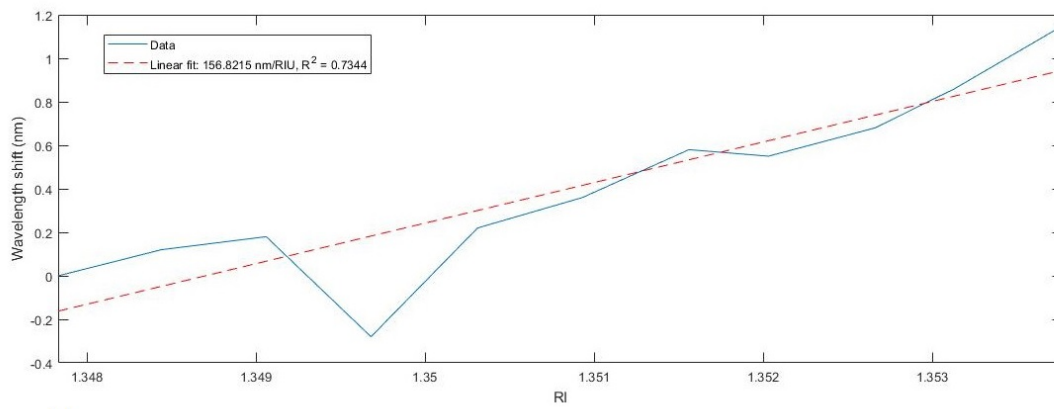


**Figure 2.8:** Tapered FOS with waist diameter  $20\mu\text{m}$  and length  $39\text{mm}$  : a) Spectrum of the wavelength shift; b) Wavelength shift as a function of the RI change

The testing result of the tapered SMF with the least obtained waist diameter  $19\mu\text{m}$  can be seen from the Figure 2.9. The product has sensitivity of  $156.8215 \text{ nm/RIU}$  and coefficient of determination  $R^2 = 0.7344$  that is the highest among the tested tapered SMFs. The sensitivity value for this particular taper can be considered as the more accurate value than for the tapered fiber with waist diameter  $25\mu\text{m}$ , since for the taper of  $25\mu\text{m}$  the measurements were conducted in steps of additional  $200\mu\text{l}$  of 40% sucrose, while for other tapers in each computation step additional  $100\mu\text{l}$  of 40% sucrose was poured into reference solution of 10% sucrose. As the result the tapers, except  $25\mu\text{m}$  taper, have more data processing, therefore more accurate value.



a)



b)

**Figure 2.9:** Tapered FOS waist diameter 19 μm: a) Spectrum of the wavelength shift; b) Wavelength shift as a function of the RI change

## 2.3 The Simulation of Light Transmission Intensity by COMSOL

The light transmission intensity simulation for the tapered microfiber with waist diameter  $19\mu\text{m}$  was conducted using COMSOL Multiphysics 5.0. The module used for simulation is RF (Radio frequency) with Electromagnetic Analysis and Frequency Domain. The geometrical model 2D (XY plane) was used to determine the flow of normal evanescent field to the cross-section area of the tapered field. The material was defined for the commercial SMF-28 with core diameter  $9.3\mu\text{m}$  and numerical aperture of 0.13. The core material was denoted as the silicon with refractive index  $n_{core} = 1.478$  and cladding made of doped silicon with refractive index  $n_{core} = 1.445$ . The mesh type was defined as the physical-controlled mesh with element size of extra fine.

The incident field frequency was defined as  $(c/\lambda)$  where  $c$  is the speed of the light in a vacuum and wave's wavelength is  $1550\text{nm}$ . Then taper was tested sensing media with different RI including 1.45, 1.47 and 1.48.

From the Figure 2.10, it can be seen that the light propagated along the core of the fiber. This is the logical output, since the refractive index of the core is higher than the sensing media RI. Despite this fact there is still some field propagation along the cladding of the fiber with low intensity.

Figure 2.11 displays the cross-section propagation of electric field within the tapered fiber for the sensing media RI = 1.47. In this case the RI of surrounding is near to the core value. Therefore, the partial loss of evanescent field can be observed.

For the case when sensing media RI is higher than the core RI, the high loss of evanescent field and more light is propagated into the surrounding, as shown in Figure 2.12.

Therefore, it can be said that with increasing of refractive index of sensing media, the light propagation to the surrounding is also increased.

## 2.4 Discussions and Recommendations

This section consists of some observations that were discovered during the fabrication and testing of the tapers. Practically, it was found that the tapered fibers with less waist diameter have higher sensibility than fibers with thick waist. However, the main issues related with narrower waist is that tapers with small diameters degrade faster and losses can increase over the time without proper maintenance. In addition, to achieve smaller waist, the speed parameter of LSS system should be increased in the same manner. For instance, to achieve a successful fabrication of the microfiber with waist diameter less than  $20\mu\text{m}$  the pulling speed of the moving holder have to be not less than  $0.48\text{ mm/s}$ . On other hand, increasing the drawing

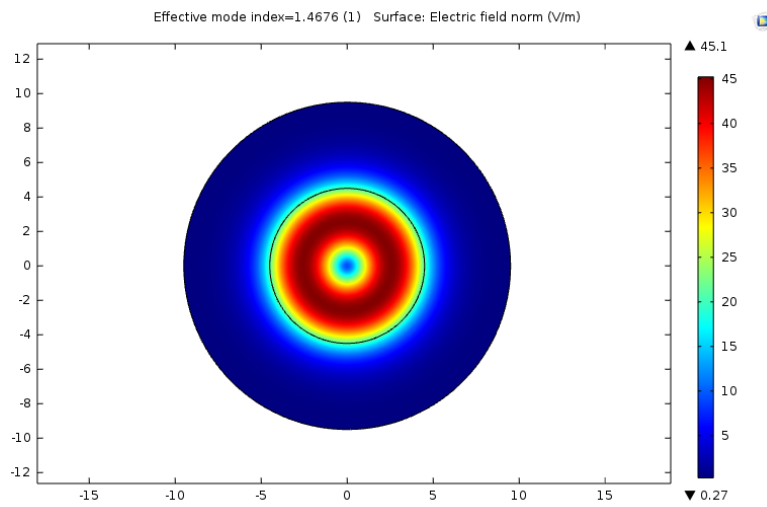


**Figure 2.10:** The cross-section propagation of the normal electric field for the sensing media RI = 1.45

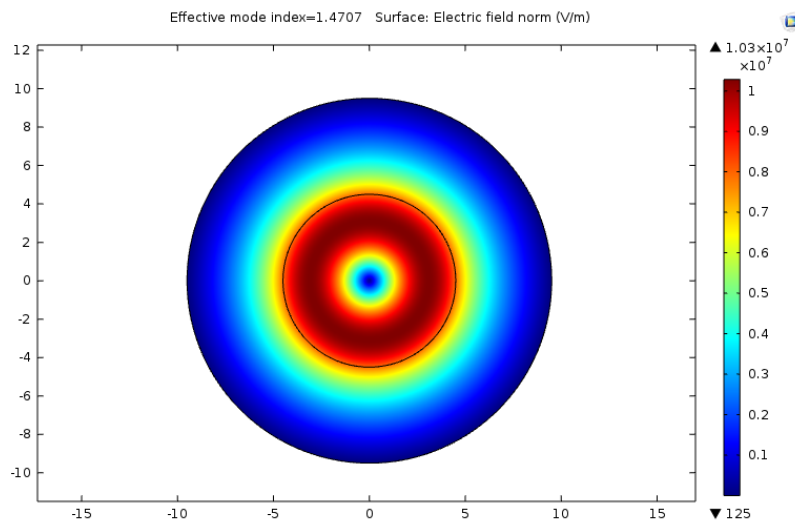


**Figure 2.11:** The cross-section propagation of the normal electric field for the sensing media RI = 1.47

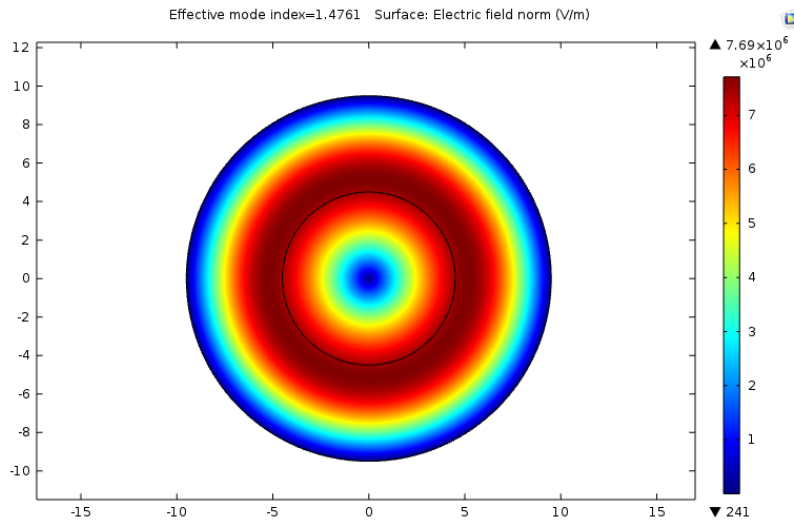


**Figure 2.12:** The cross-section propagation of the normal electric field for the sensing media RI = 1.48

speed cannot guarantee the geometric uniformity of the taper and can even break down the taper. Therefore, the least possible speed for the particular taper is more preferable, which is not always achievable, since the small waist diameter requires higher pulling speed.

Another factor that plays important role in characterization of microscale FOS is the adiabatic angle (taper angle). As it was mentioned in theoretical section, the microfibers can be considered as the adiabatic type when there is smooth transition between the uniform waist region and cladding region. This criterion mainly depends on the taper shape and length of the transition region. It was discovered that sine taper shape is more preferable than linear taper shape, for which case there is higher transitional power loss (adiabatic shape is sharper). Moreover, the prolonged transitional length also contributes to improvement of performance of the tapered fiber. The main reason for that, the taper angle becomes small with increasing of the transitional length of the tapered fiber. The viral example was shown by comparing two tapers with the same waist diameter of  $20\mu\text{m}$  but two different transitional lengths (5 and 12mm). The microfiber with longer transitional length 12mm has better external RI sensitivity than fiber with 5mm transitional length

Furthermore, the appropriate management of different LSS configuration is required for the final successful appearance of the tapered fiber. The parameters including heating condition/melting temperature, pulling speed should be properly selected by trial and error method based on the experience of working with LSS system.

During the characterization and testing of the tapered FOS, it was found that the selected testing method in terms of scattered power loss within the tapered region is susceptible noise, since it involves the demodulation of backscattered signal with low intensity. Moreover, this method cannot conduct accurate result for short-term measurements and requires long-term measurements (assembling of more data) for the detailed computation. Therefore, the investigation of tapers with other methods is recommended. For instance, the measurement of change of the effective RI in terms of the wavelength shift of the Rayleigh signature could be one of these methods, since this testing process is immune to the power fluctuations [22]. In addition, it was also recommended to carry out future examinations with other type of fibers such as multimode fibers (MMF), fibers with integrated Bragg grating (FBG) and fibers with doped nanoparticles in view of the fact that these architectures provide higher sensibility and better computation accuracy [22]. The main drawback for these type fibers is that their complexity in structure thus higher cost and availability in the market. Real time testing with biological and chemical specimen also suggested in order to realize and examine the full capability of the produced tapered FOS in practical field.

## Chapter 3

# Conclusion

In this research the fabrication process of tapered microscale FOS using heat transfer and pulling method with automatic Laser Splicing System and its characterization in terms of external RI was proposed. The main aim of the work is the successful fabrication of tapered fiber with micro scale dimensions that can substitute the present conventional sensing devices. During the fabrication, tapered fibers with various waist diameters was produced. The most successful instances within the produced fibers were selected and their test results were provided. The fiber with least waist diameter  $19\ \mu\text{m}$  was reached. The particular microfiber has sensitivity of  $156.8215\ \text{nm}/\text{RIU}$  and highest correlation with linearity among the tested tapered SMFs. It can be said that final product showed satisfying RI sensitivity and high linearity between the wavelength shift and RI change. In addition, it was concluded that the proposed method for fabrication has superiority such as simplicity in fabrication process, automatic control system, since operator does not directly involved in fabrication but provides with input parameters. Moreover, this method can provide high accuracy in fabrication and sufficient sensibility for proposed waist diameter. On other hand, the main limitation of this method is that final product mainly depends on the configuration of LSS and fabrication of smaller tapered fibers might require the long-term management of the LSS. Furthermore, the ideal linearity between the wavelength shift and RI change was not achieved. Therefore, for the technical realization of the full potential advantages of tapered microscale FOS, further research is needed, improvement of their design, organization of small-scale production and testing in real practical is required. In this case, they could significantly enrich the tools of biomedical research and medical practice.

# Bibliography

- [1] Daniele Tosi et al. "Fiber optic sensors for sub-centimeter spatially resolved measurements: Review and biomedical applications". In: *Optical Fiber Technology* 43 (2018), pp. 6–19.
- [2] Hamid Latifi et al. "Nonadiabatic tapered optical fiber for biosensor applications". In: *Photonic Sensors* 2.4 (2012), pp. 340–356.
- [3] Marie Pospíšilová, Gabriela Kuncová, and Josef Trögl. "Fiber-optic chemical sensors and fiber-optic bio-sensors". In: *Sensors* 15.10 (2015), pp. 25208–25259.
- [4] Li-wei Li and Xiao-hong Sun. "Investigation on the tapered fiber evanescent-field sensor based on the Comsol software". In: *2012 Symposium on Photonics and Optoelectronics*. IEEE. 2012, pp. 1–3.
- [5] Yun-Jiang Rao. "In-fibre Bragg grating sensors". In: *Measurement science and technology* 8.4 (1997), p. 355.
- [6] S Al-Askari et al. "Optimizing tapered microfiber sensor design and simulation". In: *ARPJ Journal of Engineering and Applied Sciences* 11.1 (2016), pp. 449–452.
- [7] Wanvisa Talataisong, Rand Ismaeel, and Gilberto Brambilla. "A review of microfiber-based temperature sensors". In: *Sensors* 18.2 (2018), p. 461.
- [8] Hans-Curt Flemming et al. "Biofilms: an emergent form of bacterial life". In: *Nature Reviews Microbiology* 14.9 (2016), p. 563.
- [9] Hans-Curt Flemming and Jost Wingender. "The biofilm matrix". In: *Nature reviews microbiology* 8.9 (2010), pp. 623–633.
- [10] Philip Hunter. "The mob response". In: *EMBO reports* 9.4 (2008), pp. 314–317.
- [11] Marc Habash and Gregor Reid. "Microbial biofilms: their development and significance for medical device—related infections". In: *The Journal of Clinical Pharmacology* 39.9 (1999), pp. 887–898.
- [12] Tatsaporn Todhanakasem. "Microbial biofilm in the industry". In: *Afr J Microbiol Res* 7.17 (2013), pp. 1625–1634.
- [13] T Reg Bott. *Industrial biofouling*. Elsevier, 2011.

- [14] Matthias Fischer, Martin Wahl, and Gernot Friedrichs. "Design and field application of a UV-LED based optical fiber biofilm sensor". In: *Biosensors and Bioelectronics* 33.1 (2012), pp. 172–178.
- [15] Yong Yuan et al. "Electrochemical surface plasmon resonance fiber-optic sensor: in situ detection of electroactive biofilms". In: *Analytical chemistry* 88.15 (2016), pp. 7609–7616.
- [16] Haluk Beyenal et al. "Fiber-optic microsensors to measure backscattered light intensity in biofilms". In: *Applied optics* 39.19 (2000), pp. 3408–3412.
- [17] Dandan Sun et al. "Label-Free Thrombin Detection Using a Tapered Fiber-Optic Interferometric Aptasensor". In: *Journal of Lightwave Technology* 37.11 (2018), pp. 2756–2761.
- [18] Yanping Xu et al. "Recent developments in micro-structured fiber optic sensors". In: *Fibers* 5.1 (2017), p. 3.
- [19] Misha Sumetsky. "Theory of adiabatic optical fiber and microfiber tapers". In: *Optical Fiber Communication Conference*. Optical Society of America. 2006, OTuH2.
- [20] Limin Tong. "Micro/nanofibre optical sensors: challenges and prospects". In: *Sensors* 18.3 (2018), p. 903.
- [21] Qi Wang et al. "High sensitivity refractive index sensor based on splicing points tapered SMF-PCF-SMF structure Mach-Zehnder mode interferometer". In: *Sensors and Actuators B: Chemical* 225 (2016), pp. 213–220.
- [22] Marzhan Sypabekova et al. "Fiber optic refractive index sensors through spectral detection of Rayleigh backscattering in a chemically etched MgO-based nanoparticle-doped fiber". In: *Optics letters* 43.24 (2018), pp. 5945–5948.